atmosphere

MDPI

Article

Strategy for the Prediction of Typhoon Wind and Storm Surge Height Using the Parametric Typhoon Model: Case Study for Hinnamnor in 2022

Jun-Hyeok Son, Hojin Kim *, Ki-Young Heo, Jae-Il Kwon *, Sang-Hun Jeong, Jin-Yong Choi, Je-Yun Chun, Yeong-Yeon Kwon and Jung-Woon Choi

Korea Institute of Ocean Science & Technology, Busan 49111, Republic of Korea
* Correspondence: kimhojin@kiost.ac.kr (H.K.); jikwon@kiost.ac.kr (J.-I.K.)

Abstract: The parametric typhoon model is a powerful typhoon prediction and reproduction tool with advantages in accuracy, and computational speed. To simulate typhoons' horizontal features, the longitude and latitude of the typhoon center, central pressure, radius of maximum wind speed (Rmax), and background states (such as surface air pressure and wind speed) are required. When a typhoon approaches or is predicted to affect Korea, the Korea Meteorological Agency (KMA) notifies the above-mentioned parameters, except for the Rmax and background state. The contribution of background wind and pressure is not very significant; however, Rmax is essential for calculating typhoon winds. Therefore, the optimized Rmax for the typhoons over the past five years was estimated at each time step compared with the in situ wind observation record. After that, a fifth-order polynomial fitting was performed between the estimated Rmax and the radius of strong wind (RSW; >15 m/s) provided by the KMA. Finally, the Rmax was calculated from the RSW via the empirical equation, and the horizontal fields of typhoon Hinnamnor (2211) were reproduced using a parametric model. Furthermore, the ocean storm surge height was adequately simulated in the surge model.

Keywords: typhoon; parametric typhoon model; storm surge; radius of maximum wind speed; Hinnamnor

Citation: Son, J.-H.; Kim, H.; Heo, K.-Y.; Kwon, J.-I.; Jeong, S.-H.; Choi, J.-Y.; Chun, J.-Y.; Kwon, Y.-Y.; Choi, J.-W. Strategy for the Prediction of Typhoon Wind and Storm Surge Height Using the Parametric Typhoon Model: Case Study for Hinnamnor in 2022. *Atmosphere* **2023**, *14*, 82. https://doi.org/10.3390/atmos14010082

Academic Editors: Ching-Yuang Huang, Shu-Ya Chen and Kao-Shen Chung

Received: 21 November 2022
Revised: 25 December 2022
Accepted: 29 December 2022
Published: 31 December 2022

1. Introduction

Typhoon forecasting with high accuracy is required to reduce social and financial damage. Since a typhoon accompanies various extreme atmospheric-ocean phenomena, the typhoon itself can be a cause of compound hazards around Western Pacific. Typhoon intensity and track are critical concerns in the coastal regions during boreal summer and autumn due to torrential rainfall, vigorous winds, storm surges, and oceanic waves [1–3]. Typhoon tracks are known to be mainly determined by beta drift [4], and background steering winds [5]. In addition to those, land surface friction, and other atmospheric conditions over land and ocean affect the typhoon tracks [6–8]. The intensity is influenced by vertical wind shear [9,10], oceanic thermodynamic conditions [11–13], and the internal dynamics of the typhoon itself [14]. Despite the remarkable advancements in the scientific knowledge of typhoons, current dynamical models for numerical prediction still have large uncertainties for typhoon forecasts. Therefore, for a more reliable typhoon forecast, many operational numerical weather forecasting agencies, including the Korea Meteorological Agency (KMA; https://www.weather.go.kr/w/typhoon/report.do), provide probability notifications for the track and impact radius of typhoons via ensemble dynamical model simulations [15,16].

When a typhoon forecast is performed, information such as the typhoon location (°E and °N), radius (km) of strong winds (RSW; >15 m/s), and minimum pressure (hPa) is announced by the operational administration center based on the operational forecasting

model output. The specific parameters representing typhoon characteristics are estimated using sophisticated numerical ensemble modeling results, which are the most reliable and best output at each moment. Meanwhile, Thompson and Cardone [17] developed a parametric typhoon model to generate two-dimensional horizontal fields of surface wind and pressure from the typhoon information announced by the operational center. At first, the parametric typhoon model was developed and used for recreating hurricane winds in the Atlantic basin and those affecting the USA [17]. After that, this model was broadly applied for both research and operational purposes, even on other basins such as Indian Ocean basin [18], and Western Pacific [19]. This diagnostic method has the advantage in accuracy compared to the use of direct typhoon simulation data attained from a member of the ensemble simulations.

The parametric typhoon model is based on the basic vortex model [17,20,21], and its essence is the reproduction of horizontal pressure fields and pressure gradient force, generating horizontal surface winds. The parametric typhoon model calculates pressure as follows [22,23]:

$$p(r) = p_0 + \Delta p e^{-R_{max}/r} \quad (1)$$

where p is the pressure field representing the typhoon, p_0 is the pressure at the typhoon center (minimum pressure), Δp is the pressure difference between the minimum and background normal conditions. Rmax is the radius of the maximum wind, and r is the distance from the typhoon center.

When a typhoon approaches Korea or is predicted to propagate toward Korea, typhoon information is noticed on the KMA website. The predicted typhoon location and minimum pressure are listed at each time step until the typhoon turns into an extratropical cyclone. However, there is no information about the Rmax, which is the distance from the typhoon's center to the point of maximum wind speed (Figure 1). As shown in Equation (1), Rmax is an essential parameter to reconstruct the horizontal structure of a typhoon pressure field.

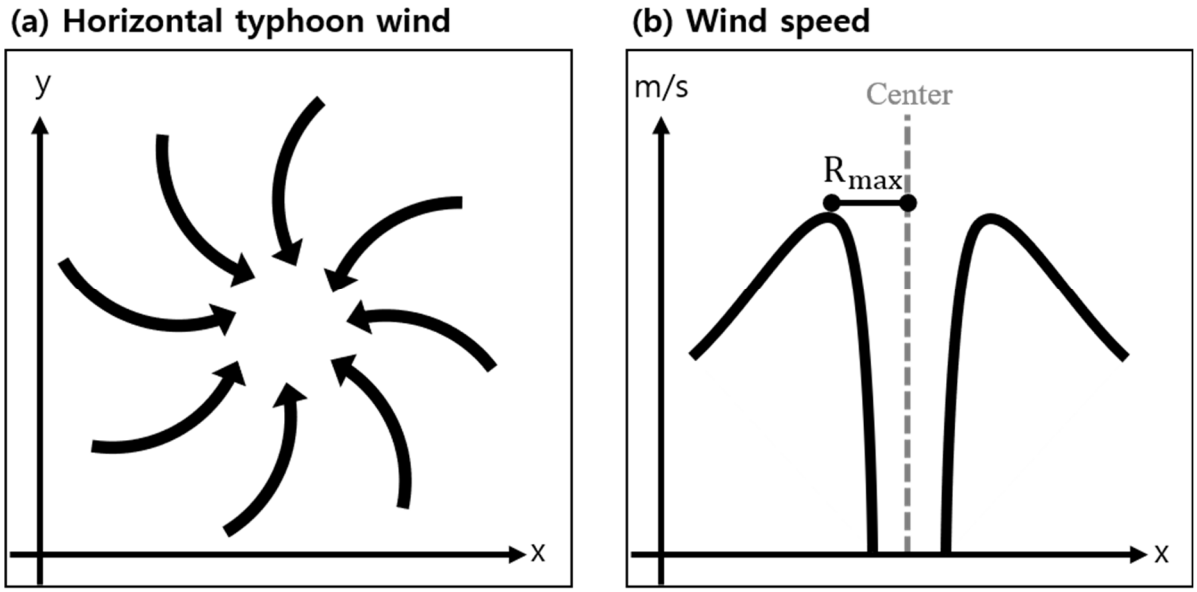

Figure 1. Schematic diagram for the typhoon horizontal wind structures (**a**), and wind speed (**b**).

The Rmax can be obtained by direct measurement using an aircraft, estimated from satellite images, and other empirical methods [24–28]. However, for near real-time prediction, the Rmax estimation from the parameters announced by the KMA is the simplest and best way, if that is possible. Therefore, in this study, we propose a strategy for estimating the Rmax from RSW to predict the two-dimensional characteristics of typhoons.

2. Data and Methods

The surface wind in the fifth generation of the atmospheric reanalysis dataset [29] from the European Center for Medium-Range Weather Forecasts (ERA5) from 1981 to 2020 was extracted to calculate the daily wind climatology. In situ wind speed observations were downloaded from the KMA data portal website (https://data.kma.go.kr/resources/html/en/aowdp.html, accessed on 15 September 2022) and the KIOST website (https://kors.kiost.ac.kr/en/). For the validation of the storm surge height, sea surface height data were downloaded from the Korea Hydrographic and Oceanographic Agency (KHOA) website (http://www.khoa.go.kr/hightide/). The locations of the in situ observation and variables are shown in Figure 2. The datasets measured in every location, as shown in Figure 2, have been available since 2019 for KIOST, 2016 for KHOA, and 2015 for KMA. Therefore, it was decided to conduct an analysis using the data since 2018, considering the recent number of typhoons that affected Korea and the individual typhoon impact.

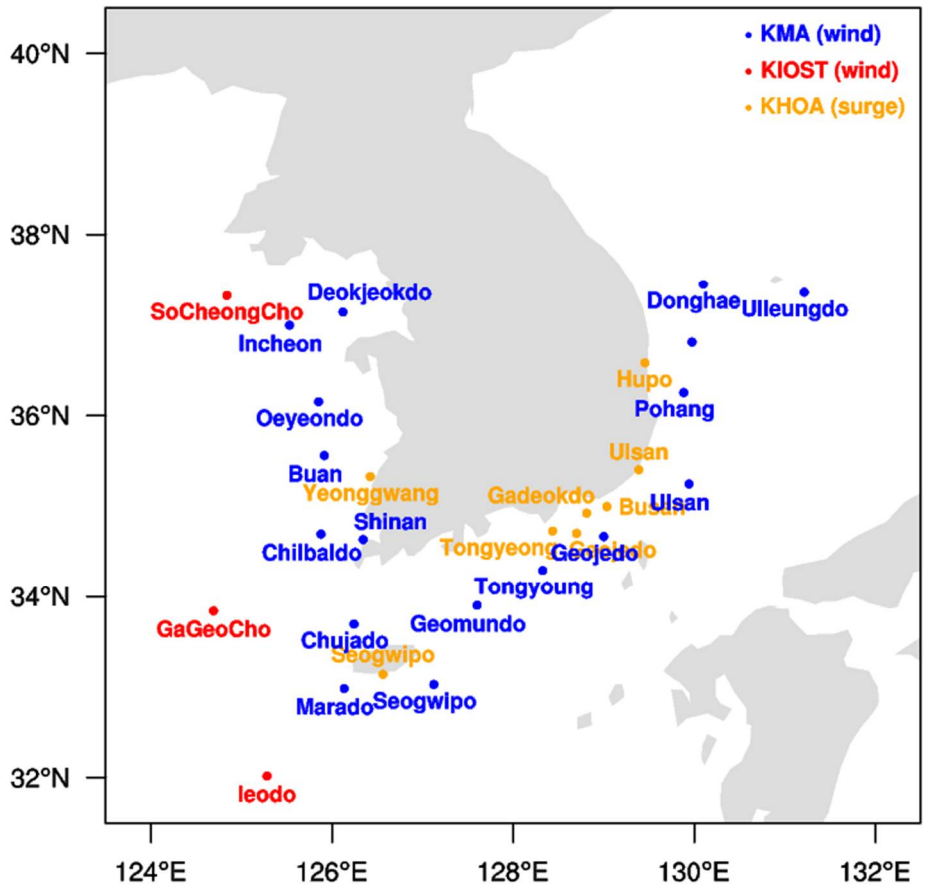

Figure 2. Observation locations of the KMA, KIOST, and KHOA from 2018 to 2022. The wind speed was observed in the KMA buoys (blue) and KIOST research stations (red). Orange dots indicate the KHOA surge height observation sites.

The southernmost point (125.18° E, 32.12° N) of the wind observation is an Ieodo Ocean Research Station (Figure 2), located 149 km southwest of Jeju Island in Korea [30,31] (on the path of most typhoons approaching Korea). In general, the radius of a small typhoon is approximately 200 km, and 1°N is approximately 96 km. Therefore, typhoons affecting Korea were selected as typhoons located north of 30° N.

3. Estimation of the Radius of Maximum Wind Speed

In the previous study, Rmax calculation methods from typhoon central pressure, the meridional location of the typhoon, migration speed, and maximum wind in climatological typhoon information were suggested [28,32]. The empirical formula derived from the

climatological characteristics of typhoons is similar to the multivariable linear regression method. This approach is very efficient; however, the variables used as input data in mid-latitudes (>30° N) are often significantly correlated, and show a low correlation with Rmax. This means that higher-order polynomials rather than a linear formula should be used, and the multivariable method may not be needed to be considered.

First, for the statistical estimation of Rmax, we need to determine the optimized Rmax for each typhoon affecting Korea based on the parametric typhoon model. For that, the model simulation was repeated, with increasing Rmax from 30 to 120 km at 1 km intervals for 22 typhoons affecting Korea from 2018 to 2022, excluding typhoon Hinnamnor (Table 1). The model domain was 117°–135° N and 25°–44° N, with a 0.083° horizontal interval and a time step of 1 hour. After the iteration of the model simulation, the simulated surface wind speeds were compared to in situ KMA (17 observation points) and Korea Institute of Ocean Science and Technology (KIOST; 3 observation points) wind speed observations in the oceans surrounding Korea (Figure 2). Over land, the wind speed reduces due to drag and friction; however, the parametric typhoon model does not consider these processes. Therefore, for a fair comparison, only the data at ocean sites were used.

Table 1. Information on typhoons affecting Korea from 2018 to the summer of 2022 based on the KMA best track. The numbers in parentheses beside typhoon names show the order (NN) of typhoon in each year (YY). The time is estimated as Korean standard time (KST), which is UTC+09 hour.

Name (YYNN)	Generation (KST)	When latitude > 30°N	Termination
Prapiroon (1807)	2018-06-28 21:00	2018-07-03 00:00	2018-07-04 18:00
Rumbia (1818)	2018-08-15 15:00	2018-08-16 15:00	2018-08-18 09:00
Soulik (1819)	2018-08-16 03:00	2018-08-22 09:00	2018-08-25 03:00
Trami (1824)	2018-09-21 03:00	2018-09-30 09:00	2018-10-01 15:00
Kong-rey (1825)	2018-09-28 15:00	2018-10-05 18:00	2018-10-07 09:00
Danas (1905)	2019-07-16 09:00	2019-07-19 15:00	2019-07-21 21:00
Francisco (1908)	2019-08-01 21:00	2019-08-05 09:00	2019-08-07 21:00
Lekima (1909)	2019-08-04 15:00	2019-08-10 15:00	2019-08-12 21:00
Krosa (1910)	2019-08-06 09:00	2019-08-14 21:00	2019-08-16 21:00
Lingling (1913)	2019-09-01 21:00	2019-09-06 18:00	2019-09-08 09:00
Tapah (1917)	2019-09-18 09:00	2019-09-22 06:00	2019-09-23 09:00
Mitag (1918)	2019-09-26 21:00	2019-10-01 21:00	2019-10-03 12:00
Jangmi (2005)	2020-08-09 03:00	2020-08-10 03:00	2020-08-10 17:00
Bavi (2008)	2020-08-22 09:00	2020-08-25 18:00	2020-08-27 15:00
Maysak (2009)	2020-08-28 03:00	2020-09-02 06:00	2020-09-03 12:00
Haishen (2010)	2020-09-01 09:00	2020-09-06 18:00	2020-09-07 21:00
Lupit (2109)	2021-08-03 09:00	2021-08-08 15:00	2021-08-09 09:00
Omais (2112)	2021-08-15 09:00	2021-08-23 12:00	2021-08-24 06:00
Chanthu (2114)	2021-09-06 21:00	2021-09-13 15:00	2021-09-18 09:00
Aere (2204)	2022-07-01 03:00	2022-07-04 09:00	2022-07-05 03:00
Songda (2205)	2022-07-27 03:00	2022-07-30 03:00	2022-08-01 09:00
Trases (2206)	2022-07-31 12:00	2022-08-01 03:00	2022-08-01 21:00
Hinnamnor (2211)	2022-08-28 15:00	2022-09-05 12:00	2022-09-06 21:00

Figure 3 shows the root mean square error (RMSE) between the observational surface wind speed of each typhoon located north of 30°N and the parametric typhoon model outputs with the prescribed Rmax ranging from 30 to 120 km. The individual gray line

shows the RMSE at every time step, and the red line shows the time average. The minimum value of the RMSE at each line was selected for the optimized Rmax. Consequently, the Rmax varied in each typhoon case and at each time step [33]. Here, the optimized Rmax tended to decrease when typhoons approached Korea due to a decrease in typhoon energy with a smaller horizontal size and weaker intensity in general. The Rmax was larger in the subtropics, when the typhoon was more intense and larger than that located at midlatitudes.

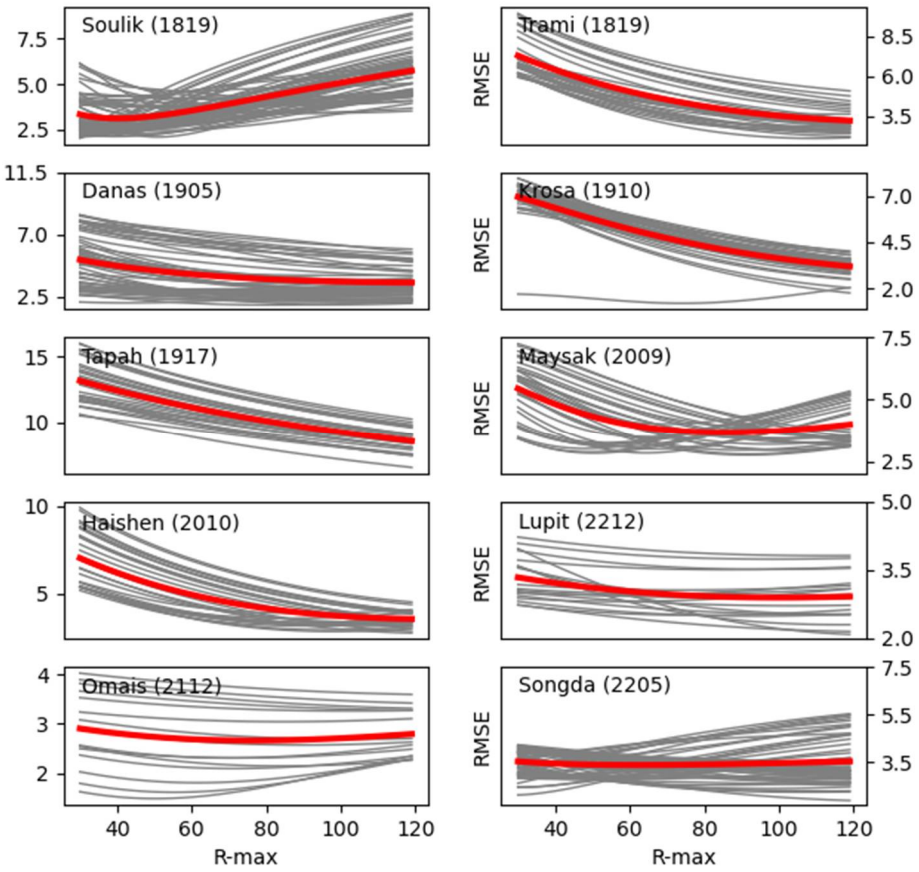

Figure 3. Root mean square error (RMSE) between observational surface wind speed and parametric typhoon model output with variations of typhoon Rmax. Y-axis denotes RMSE (m/s), and x-axis shows Rmax (km). Of the 23 typhoon cases, only 10 results are plotted as examples.

Twenty-three typhoons directly impacted Korea from 2018 to the summer of 2022; however, only 22 typhoons, excluding Hinnamnor (2211), were analyzed for the calculation of RMSE and Rmax estimation. In Figure 3, the RMSE of typhoons Soulik (1819), Trami (1824), Danas (1905), Krosa (1910), Tapah (1917), Maysak (2009), Haishen (2010), Lupit (2109), Omais (2112), and Songda (2205) are shown as examples. One of the strongest typhoons, Hinnamnor (2211), was analyzed as the validation case. The estimated optimal Rmax from the parametric model simulations showed no significant correlation with RSW (R = 0.22). Here, a correlation coefficient indicated a linear relationship. Therefore, to apply a higher-order non-linear relationship between Rmax and RSW, polynomial fitting was used to calculate Rmax from RSW. The number of samples used for polynomial fitting for each typhoon was not selected equally due to the different lifetime and migration speeds of individual typhoons. The least-squares error polynomial fitting result between the estimated Rmax and RSW is as follows:

$$R_{max} = 1.764e^{-11} \times RSW^5 - 1.912e^{-8} \times RSW^4 + 9.149e^{-6} \times RSW^3 - 0.002306 \times RSW^2 + 0.2844 \times RSW + 65.92 \quad (2)$$

The correlation coefficient between the calculated Rmax from RSW via Equation (2) and the estimated Rmax from the RMSE of the observational surface wind speed was approximately 0.37 for the number of ~2200 samples (22 typhoons, and 100 timesteps on average). For example, the polynomials, including typhoon Hinnamnor, were not significantly different from Equation (2) (not shown). One thing to note is that the order of polynomials should be odd because of the semi-linear relationship between Rmax and RSW.

4. Simulation of Hinnamnor Surface Wind and Storm Surge Height

For the simulation of typhoon surface wind, the KMA best track data (Table 2) and the estimated Rmax via Equation (2) were used in the parametric typhoon model simulation for Hinnamnor (2211). The climatological daily mean surface wind fields of ERA5 atmospheric reanalysis data were used as the background wind (Figure 4a). The climatological surface wind speed was less than 5 m/s; therefore, its effect was not fatal. However, the use of the climatological background state is definitely better than the use of a non-existent background wind field or a random constant value. The simulated horizontal wind and pressure features of Hinnamnor on 5 September 2022 are shown in Figure 4b. The intense wind speeds when the typhoon arrived are well-matched with the in situ observations at Geojedo (Figure 4c). Other wind observation location results near the typhoon center show similar results to the Geojedo data (not shown); however, there is a large difference in wind speed far from the typhoon center. The wind speed simulation before the typhoon arrival tends to be incorrect due to the absence of the other atmospheric phenomena such as midlatitude synoptic disturbance or typhoon generating Rossby waves.

Table 2. Input parameters of Hinnamnor (2211) for the parametric typhoon model.

Date (KST)	Latitude (°N)	Longitude (°E)	Center Pressure (hPa)	Radius of Strong Wind (km)
2022-08-28 15:00	25.8	149.5	1004	-
2022-08-28 21:00	26.9	148.5	998	220
2022-08-29 3:00	27.2	147	994	220
2022-08-29 9:00	27.3	145.2	985	230
2022-08-29 15:00	27.4	143.3	980	260
2022-08-29 21:00	27.3	141.2	965	280
2022-08-30 3:00	27.1	139.3	965	300
2022-08-30 9:00	26.8	137.3	945	300
2022-08-30 15:00	26.8	135.4	925	300
2022-08-30 21:00	26.5	133.6	915	300
2022-08-31 3:00	26.3	131.9	915	230
2022-08-31 9:00	25.9	130.3	915	240
2022-08-31 15:00	25.4	129	915	250
2022-09-01 3:00	23.7	126.4	915	280
2022-09-01 15:00	21.8	125.5	920	300
2022-09-01 21:00	21.3	125.5	920	320
2022-09-02 3:00	21.3	125.5	925	320
2022-09-02 9:00	21.5	125.4	935	340
2022-09-02 15:00	21.9	125.1	935	360
2022-09-02 21:00	22.2	124.8	935	360

Table 2. *Cont.*

Date (KST)	Latitude (°N)	Longitude (°E)	Center Pressure (hPa)	Radius of Strong Wind (km)
2022-09-03 3:00	22.5	124.7	940	400
2022-09-03 9:00	23	124.6	940	410
2022-09-03 15:00	23.6	124.6	940	420
2022-09-03 21:00	24.3	124.8	940	430
2022-09-04 3:00	25.1	124.6	940	430
2022-09-04 9:00	26	124.5	940	430
2022-09-04 15:00	27	124.8	935	430
2022-09-04 21:00	27.7	124.6	935	430
2022-09-05 3:00	28.6	124.7	935	430
2022-09-05 6:00	29.2	124.8	935	430
2022-09-05 9:00	29.8	124.9	930	430
2022-09-05 12:00	30.2	125.1	930	430
2022-09-05 15:00	31	125.6	935	430
2022-09-05 18:00	31.7	126.1	940	430
2022-09-05 21:00	32.4	126.6	940	420
2022-09-06 0:00	33.3	127.3	945	410
2022-09-06 3:00	34.2	128	950	400
2022-09-06 6:00	35.2	129.2	955	400
2022-09-06 9:00	36.5	130.5	965	390
2022-09-06 12:00	37.8	131.6	970	370
2022-09-06 15:00	39.3	133	975	280
2022-09-06 18:00	42	135.7	975	280
2022-09-06 21:00	44.4	136.7	980	-

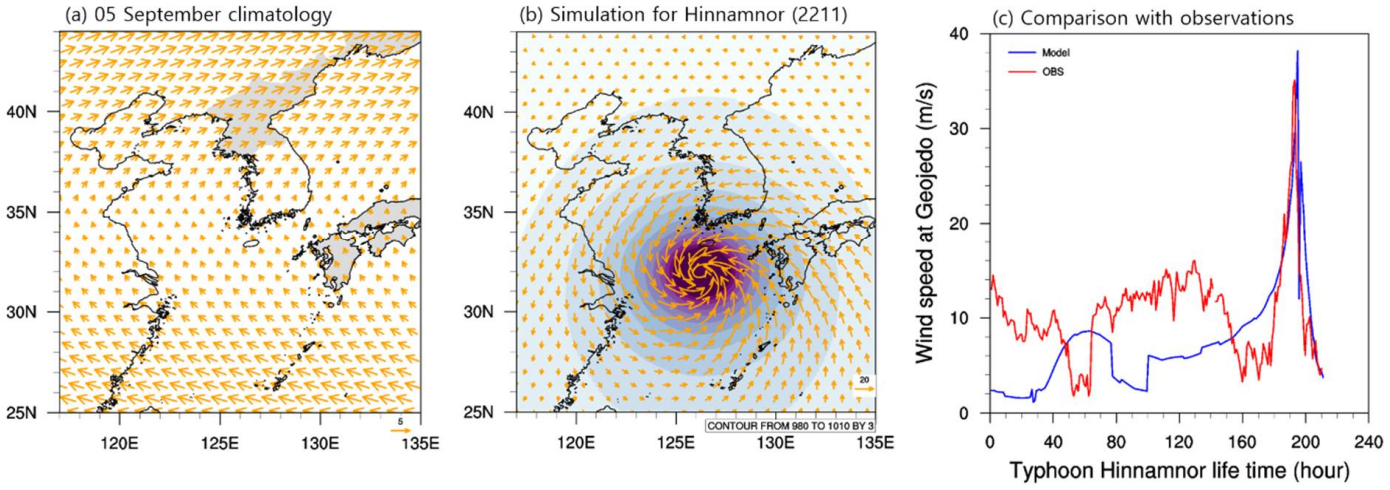

Figure 4. (**a**) Daily climatological mean surface wind, (**b**) T-P model simulation for Hinnamnor (snapshot on 5 September). The reference vector shows 5 m/s in (**a**) and 20 m/s in (**b**). Wind speed simulation (blue line) and in situ observations (red line) at Geojedo are shown in (**c**).

As an implication of the parametric typhoon model results, the simulated pressure and wind data were prescribed as input data for the storm surge model simulation [19,34]. Here,

the Korea Ocean Research and Development Institute-Storm surge model (KORDI-S) [35] was used. Realistic and accurate wind and pressure input data are needed to predict storm surges precisely [36]. Using the parametric typhoon model results for Hinnamnor, the storm surge height was simulated and validated for Busan, Gadeokdo, Geojedo, Ulsan, Tongyeong, Teonggwang, Seogwipo, and Hupo (orange dots in Figure 2), as shown in Figure 5. The KORDI-S model simulation results tended to overestimate the surge height compared to the observations; however, they matched well, particularly in Busan, Gadeokdo, and Ulsan. The overestimation may be caused by the intense simulation of wind speed due to the absence or coarse resolution of topography (topography is not considered in the parametric typhoon model, and the horizontal resolution of topography is ~1.8 km in the surge model) and asymmetric horizontal structure of typhoon in real observations (if the background state is considered zero, the parametric typhoon model output is perfectly symmetrical in a horizontal structure). In addition, the uncertainty in RSW can contribute to both polynomials, as shown in Equation (2) and final prediction of Rmax [37].

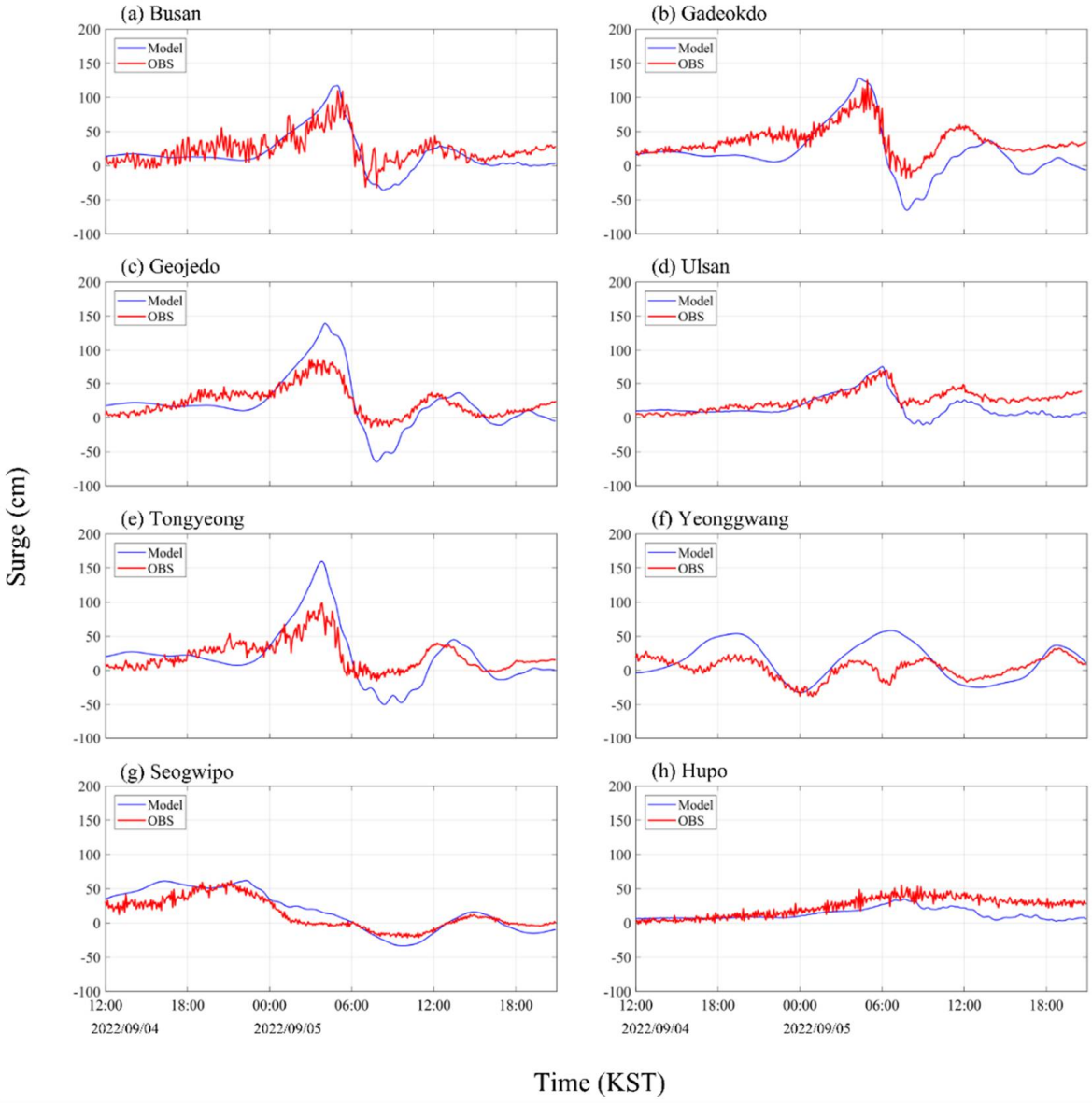

Figure 5. Surge model simulation results and KHOA observations at (**a**) Busan, (**b**) Gadeokdo, (**c**) Geojedo, (**d**) Ulsan, (**e**) Tongyeong, (**f**) Yeonggwang, (**g**) Seogwipo, and (**h**) Hupo from 4 to 5 September in 2022.

5. Conclusions and Discussion

The strategy for simulating the parametric typhoon model and storm surge model suggested in this study can be summarized as follows:

Step 1. Iterative simulation of the parametric typhoon model with Rmax ranging from 30 to 120 km.

Step 2. Identifying the optimized Rmax by comparing it with surface wind speed observations over oceans.

Step 3. Polynomial fitting of Rmax using RSW (>15 m/s), and calculation of Rmax using Equation (2).

Step 4. Simulation of parametric typhoon model and KORDI-S surge model.

For Step 1, the daily climatology of the background surface wind was prescribed for a more realistic horizontal wind simulation. In Step 4, the parametric typhoon model simulation results were used as the KORDI-S surge model input data. The observation data were finally validated for one of the strongest typhoons, Hinnamnor. The parametric typhoon model reproduced the surface wind speed at Geojedo, and the storm surge prediction results matched adequately with the ocean observations, particularly in Busan, Gadeokdo, and Ulsan. In addition, for more validation, the simulations were performed in an additional two cases: Chaba in 2016, and Soulik in 2018); as a result, the typhoons and surge height were well simulated, even in such cases (not shown).

The correlation between the estimated Rmax from wind observations in the surrounding oceans and the calculated Rmax from RSW using the fifth-order polynomial was approximately 0.37 (marginally statistically significant value at 95% confidence level). To improve the correlation skill, least-square error polynomial fitting using the polynomial of degree 20 was performed (not shown). Then the correlation increased to 0.47; however, considering the overfitting problem, using excessively high-order polynomials may be unsuitable. The correlation skill of Rmax is not very high; however, the wind and storm surge simulation results when the typhoon is located near Korea are pretty good, as shown in Figures 4 and 5. This implies that the skill mainly comes typhoons impacting Korea, and typhoons far from Korea may have low accuracy using this technique.

In this study, we used surface wind speed observations for polynomial fitting; however, the observed pressure can also be used to calculate the optimal Rmax and least-squares fitting [38]. The RSW and minimum pressure at the typhoon center showed a correlation of ~0.8. However, wind observations rarely include large measurement errors; therefore, multivariable fitting using both surface wind and pressure may provide a more stable solution. In addition, the formula must be changed if the series of procedures presented in this study is repeated for other target regions affected by tropical cyclones. Equation (2) is just one of the optimized solutions for a parametric typhoon model simulation around Korea in the last five years. This empirical polynomial was calculated based on the parametric typhoon model results. Therefore, there may be a slight difference between the calculated Rmax and those estimated from actual observations such as satellite images.

The parametric typhoon model provides the simplest way to generate two-dimensional horizontal structures with surface wind and pressure using the most reliable typhoon track and intensity prediction announced by the KMA. However, the use of only limited typhoon information causes errors because no parameters show the asymmetric structures of typhoons. The KMA performs an ensemble forecast to reduce the uncertainty of typhoon track and intensity. That means there are large errors in the individual ensemble member showing the specific typhoon features. Therefore, the parametric typhoon model is now believed to be one of the best alternative methods for filling the gap between our requirements and reality. Ultimately, we should develop a dynamic model with better typhoon simulation skills.

Author Contributions: Conceptualization, J.-H.S., K.-Y.H., J.-I.K. and J.-Y.C. (Jin-Yong Choi); Methodology, J.-H.S., S.-H.J., Y.-Y.K. and J.-W.C.; Software, J.-H.S. and J.-W.C.; Validation, J.-H.S., H.K. and K.-Y.H.; Formal analysis, J.-H.S., H.K. and J.-Y.C. (Je-Yun Chun); Investigation, J.-H.S. and H.K.;

Resources, S.-H.J.; Data curation, S.-H.J. and J.-Y.C. (Jin-Yong Choi); Writing—original draft, J.-H.S., K.-Y.H. and J.-Y.C. (Jin-Yong Choi); Visualization, J.-H.S. and H.K.; Supervision, J.-H.S. and J.-I.K. All authors have read and agreed to the published version of the manuscript.

Funding: This research was a part of the project titled 'Improvements of Ocean Prediction Accuracy using Numerical Modeling and Artificial Intelligence Technology (20180447)', and 'Establishment of the Ocean Research Station in the Jurisdiction Zone and Convergence Research' supported by the Korea Institute of Marine Science & Technology Promotion (KIMST), funded by the Ministry of Oceans and Fisheries, Korea, and 'Development of Smart Technology to Support the Collection and Management of Marine Debris (3/5)' funded by the Ministry of Oceans and Fisheries, Korea.

Institutional Review Board Statement: Not applicable.

Informed Consent Statement: Not applicable.

Data Availability Statement: All datasets analyzed in the current study are publicly available.

Acknowledgments: We would like to thank Il-Ju Moon in Jeju national university for the helpful discussion.

Conflicts of Interest: The authors declare no competing interests.

References

1. Park, D.-S.R.; Ho, C.-H.; Kim, J.-H.; Kim, H.-S. Strong landfall typhoons in Korea and Japan in a recent decade. *J. Geophys. Res. Atmos.* **2011**, *116*. [CrossRef]
2. Son, J.-H.; Heo, K.-Y.; Choi, J.-W.; Kwon, J.-I. Long-lasting upper ocean temperature responses induced by intense typhoons in mid-latitude. *Sci. Rep.* **2022**, *12*, 1–8. [CrossRef] [PubMed]
3. *Typhoon Impact and Crisis Management*; Tang, D.L.; Sui, G.; Lavy, G.; Pozdnyakov, D.; Song, Y.T.; Switzer, A.D. (Eds.) Springer: Berlin/Heidelberg, Germany, 2014; pp. 1–578.
4. Holland, G.J. Tropical cyclone motion: Environmental interaction plus a beta effect. *J. Atmos. Sci.* **1983**, *40*, 328–342. [CrossRef]
5. Son, J.-H.; Kwon, J.-I.; Heo, K.-Y. Weak upstream westerly wind attracts western North Pacific typhoon tracks to west. *Environ. Res. Lett.* **2021**, *16*, 124041. [CrossRef]
6. Wong, M.L.M.; Chan, J.C.L. Tropical Cyclone Motion in Response to Land Surface Friction. *J. Atmos. Sci.* **2006**, *63*, 1324–1337. [CrossRef]
7. Chan, J.C.L.; Liang, X. Convective Asymmetries Associated with Tropical Cyclone Landfall. Part I: *f*-Plane Simulations. *J. Atmos. Sci.* **2003**, *60*, 1560–1576. [CrossRef]
8. Fujiwhara, S. The natural tendency towards symmetry of motion and its application as a principle in meteorology. *Q. J. R. Meteorol. Soc.* **1921**, *47*, 287–292. [CrossRef]
9. Ge, X.; Li, T.; Peng, M. Effects of Vertical Shears and Midlevel Dry Air on Tropical Cyclone Developments*. *J. Atmos. Sci.* **2013**, *70*, 3859–3875. [CrossRef]
10. Kim, H.-K.; Seo, K.-H. Cluster Analysis of Tropical Cyclone Tracks over the Western North Pacific Using a Self-Organizing Map. *J. Clim.* **2016**, *29*, 3731–3751. [CrossRef]
11. Yun, K.S.; Chan, J.C.L.; Ha, K.J. Effects of SST magnitude and gradient on typhoon tracks around East Asia: A case study for Typhoon Maemi (2003). *Atmos. Res.* **2012**, *109–110*, 36–51. [CrossRef]
12. Chang, M.; Ho, C.; Chan, J.C.L.; Park, M.; Son, S.; Kim, J. The Tropical Transition in the Western North Pacific: The Case of Tropical Cyclone Peipah (2007). *J. Geophys. Res. Atmos.* **2019**, *124*, 5151–5165. [CrossRef]
13. Chang, M.; Park, D.-S.R.; Ho, C.-H. Possible Cause of Seasonal Inhomogeneity in Interdecadal Changes of Tropical Cyclone Genesis Frequency over the Western North Pacific. *J. Clim.* **2021**, *34*, 635–642. [CrossRef]
14. Sitkowski, M.; Kossin, J.; Rozoff, C.M. Intensity and Structure Changes during Hurricane Eyewall Replacement Cycles. *Mon. Weather. Rev.* **2011**, *139*, 3829–3847. [CrossRef]
15. Kim, S.; Kim, H.M.; Kay, J.K.; Lee, S.-W. Development and Evaluation of the High Resolution Limited Area Ensemble Prediction System in the Korea Meteorological Administration. *Atmosphere* **2015**, *25*, 67–83. [CrossRef]
16. Yamaguchi, M.; Sakai, R.; Kyoda, M.; Komori, T.; Kadowaki, T. Typhoon Ensemble Prediction System Developed at the Japan Meteorological Agency. *Mon. Weather Rev.* **2009**, *137*, 2592–2604. [CrossRef]
17. Thompson, E.F.; Cardone, V.J. Practical Modeling of Hurricane Surface Wind Fields. *J. Waterw. Port Coast. Ocean Eng.* **1996**, *122*, 195–205. [CrossRef]
18. Das, Y. Parametric modeling of tropical cyclone wind fields in India. *Nat. Hazards* **2018**, *93*, 1049–1084. [CrossRef]
19. Kwon, J.I.; Lee, J.C.; Park, K.S.; Jun, K.C. Comparison of Typhoon wind models based on storm surge heights induced by Typhoon Maemi. *Asia Pac. J. Atmos. Sci.* **2008**, *44*, 443–454.
20. Chow, S.H. A Study of the Wind Field in the Planetary Boundary Layer of a Moving Tropical Cyclone. Master's Thesis, New York University, New York, NY, USA, 1971.

21. Cardone, V.J.; Greenwood, C.V.; Greenwood, J.A. *Unified Program for the Specification of Hurricane Boundary Layer Winds over Surfaces of Specified Roughness*; Contract Rep. CERC-92; U.S. Army Engrs. Wtrwy-1, Experiment Station: Vicksburg, MS, USA, 1992.
22. Myers, V.A. *Characteristics of United States Hurricanes Pertinent to Levee Design for Lake Okeechobee, Florida*; Hydrometeorological Report; U.S. Weather Bureau: Silver Spring, MD, USA, 1954; Volume 32, p. 126.
23. Schloemer, R.W. *Analysis and Synthesis of Hurricane Wind Patterns over Lake Okeechobee, Florida*; Hydrometeorological Report 31; National Oceanic and Atmospheric Administration: Washington, DC, USA, 1954; p. 49.
24. Anthes, R.A. Tropical cyclones: Their evolution, structure, and effects. *Meteorol. Monogr.* **1982**, *41*, 208.
25. Hsu, S.A.; Martin, M.F., Jr.; Blanchard, B.W. An evaluation of the USACE's deep water wave prediction techniques under hurricane conditions during Georges in 1998. *J. Coast. Res.* **2000**, *16*, 823–829.
26. Hsu, S.A.; Babin, A. Estimating the radius of maximum winds via satellite during hurricane LILI (2002) over the Gulf of Mexico. *Natl. Weather Assoc.* **2005**, *6*, 1–6.
27. Kieu, C.Q. An investigation into the contraction of the hurricane radius of maximum wind. *Meteorol. Atmos. Phys.* **2011**, *115*, 47–56. [CrossRef]
28. Liu, F.; Sasaki, J. Hybrid methods combining atmospheric reanalysis data and a parametric typhoon model to hindcast storm surges in Tokyo Bay. *Sci. Rep.* **2019**, *9*, 1–10. [CrossRef] [PubMed]
29. Hersbach, H.; Bell, B.; Berrisford, P.; Hirahara, S.; Horanyi, A.; Muñoz-Sabater, J.; Nicolas, J.; Peubey, C.; Radu, R.; Schepers, D.; et al. The ERA5 global reanalysis. *Q. J. R. Meteorol. Soc.* **2020**, *146*, 1999–2049. [CrossRef]
30. Kim, Y.S.; Jang, C.J.; Noh, J.H.; Kim, K.-T.; Kwon, J.-I.; Min, Y.; Jeong, J.; Lee, J.; Min, I.-K.; Shim, J.-S.; et al. A Yellow Sea Monitoring Platform and Its Scientific Applications. *Front. Mar. Sci.* **2019**, *6*, 601. [CrossRef]
31. Ha, K.-J.; Nam, S.; Jeong, J.-Y.; Moon, I.-J.; Lee, M.; Yun, J.; Jang, C.J.; Kim, Y.S.; Byun, D.-S.; Heo, K.-Y.; et al. Observations Utilizing Korea Ocean Research Stations and their Applications for Process Studies. *Bull. Am. Meteorol. Soc.* **2019**, *100*, 2061–2075. [CrossRef]
32. Knaff, J.A.; Sampson, C.R.; DeMaria, M.; Marchok, T.P.; Gross, J.M.; McAdie, C.J. Statistical Tropical Cyclone Wind Radii Prediction Using Climatology and Persistence. *Weather Forecast.* **2007**, *22*, 781–791. [CrossRef]
33. Weatherford, C.L.; Gray, W.M. Typhoon Structure as Revealed by Aircraft Reconnaissance. Part I: Data Analysis and Climatology. *Mon. Weather Rev.* **1988**, *116*, 1032–1043. [CrossRef]
34. Moon, I.-J.; Kwon, J.-I.; Lee, J.-C.; Shim, J.-S.; Kang, S.K.; Oh, I.S.; Kwon, S.J. Effect of the surface wind stress parameterization on the storm surge modeling. *Ocean Model.* **2009**, *29*, 115–127. [CrossRef]
35. Lee, J.C.; Kwon, J.I.; Park, K.S.; Jun, K.C. Calculations of storm surges, Typhoon Maemi. *J. Korean Soc. Coast. Ocean Eng.* **2008**, *20*, 93–100.
36. Jelesnianski, C.P. A numerical calculation of storm surges induced by a tropical storm impinging on a continental shelf. *Mon. Weather Rev.* **1965**, *93*, 343–358. [CrossRef]
37. Kim, H.-J.; Moon, I.-J.; Oh, I. Comparison of Tropical Cyclone Wind Radius Estimates between the KMA, RSMC Tokyo, and JTWC. *Asia-Pac. J. Atmos. Sci.* **2022**, *58*, 563–576. [CrossRef]
38. Toyoda, M.; Mori, N.; Yoshino, J. Optimization of empirical typhoon model considering the difference of radius between pressure gradient and wind speed distributions. *Coast. Eng. J.* **2022**, *64*, 376–386. [CrossRef]